7-16-1987

Channel Plate Detection in Low Energy Scanning Electron Microscopy

H. F. Helbig
Clarkson University

R. D. Rydgren
Clarkson University

L. Kotorman
IBM General Technology Division

Recommended Citation

Utah State University
MERRILL-CAZIER LIBRARY

CHANNEL PLATE DETECTION IN LOW ENERGY SCANNING ELECTRON MICROSCOPY

H.F. Helbig[1*], R.D. Rydgren[1], L. Kotorman[2]

[1]Physics Department, Clarkson University, Potsdam, New York 13676

[2]IBM General Technology Division, Essex Junction, VT 05452

Abstract

Microchannel plate (MCP) electron detectors compare favorably with the Everhart-Thornley detector for producing SEM images from both secondary and backscattered electrons. The MCP is a compact array of 10^5 - 10^6 channel electron multipliers with a gain in excess of 10^6 and the collective ability to count $\sim 10^8$ electrons per second. The MCP can be mounted coaxially with the beam allowing un–tilted sample orientation and electron collection into a large, field-free solid angle. The speed and low noise of the MCP allow images to be made in less than one second at moderate beam currents or in longer times with very low beam currents. Because of the wide detection angle, images from coaxially located MCP's show little loss of detail due to shadowing but by the same token are peculiarly "flat" in appearance. This suggests that they might usefully complement another detector in many applications. Lifetime data are still limited, but the detectors used for this report show no noticeable deterioration with well over 100 hours of use.

*Address for Correspondence:
Physics Department
Clarkson University
Potsdam, NY 13676
Phone No. (315) 268-2348

Introduction

The recent movement toward low energy scanning electron microscopy [6] has been motivated by the realization that low energy electron beams can be used to image samples which would be damaged or altered by the high energy electrons used in conventional Scanning Electron Microscopes (SEM). An important instance is the observation of functioning microcircuit elements wherein the logic state of the elements can be detected due to the effect of their voltage on the release of secondary electrons. This is known as voltage contrast. A logic gate at +5 V, for example, is very effective in retarding the emission of secondary electrons whose energy distribution peaks between 1 and 2 eV for most surfaces. The logic gate, consequently, appears dark on an SEM image whereas the same gate at ground will have no effect on the secondaries and appear bright. We have included an example of such a voltage contrast picture in Figure 1 which was made with a conventional, Everhart–Thornley detector using elaborate image enhancement techniques.

To capitalize on this potentially valuable diagnostic method, many problems associated with transporting and focussing low energy electron beams have been overcome [7]. Here we report the results of an effort to reduce the distances which the beam electrons must travel from the final lens to the sample and which the secondaries must travel from the sample to the detector.

The approach used was to supplement or replace the Everhart-Thornley (ET) detector [2], which is located to the side of the beam and the sample, with a microchannel plate (MCP) detector coaxial with the beam and just above the sample. Although there are reports of this SEM detection scheme dating back to 1972, (Griffiths et al [3], Robinson [8], Russel [10], Rosch [9], Russel and Mancuso [11]), it has not been commonly adopted and there is still relatively little information available, especially concerning the latest MCP devices.

The advantages of this coaxial geometry are largely related to the fact that, in most cases, the sample need no longer be tilted with respect to the beam and may therefore be mounted closer to the final lens and sample. If the MCP detector could be shown to provide satisfactory

images, the following improvements might be expected:

1) Stray fields would have a shorter path over which to disturb the beam focus and the collection of secondary electrons. 2) The MCP detector subtends a large solid angle from the beam spot; hence a large fraction of the secondaries would reach the detector unassisted by an electric field to guide them. The absence of a collection field would contribute further to a distortion-free beam focus. 3) Planar samples, too large to be mounted obliquely, would be easily accommodated when mounted perpendicular to the beam since they would no longer encroach on the lens structure. 4) It would become possible to position large samples for inspection by moving them in the plane perpendicular to the beam rather than obliquely. 5) The entire energy spectrum of the secondary electrons would be collected independent of their angular distribution thereby permitting more accurate metrological inspections and voltage measurements. 6) Angle-dependent phenomena could be studied by using an appropriately configured MCP.

The results of the study have been encouraging. In fact, there are strong indications that the electronic characteristics of the MCP detector may overshadow its geometric advantages.

The Detector

The detector used was a Galileo model 3025 Low Profile MCP detector. It consists of two impedance-matched circular microchannel plates in series electrically, and joined together to form a single resistive element. This is housed in a short cylindrical can as indicated in Figure 2. The construction and characteristics of similar detectors have been described by Wiza [12], Rosch [9], Robinson [8], Russel [10][11], Griffiths [3]. The detector entrance is covered by a high–transmission grid which may be biased or grounded as desired. A 6mm O.D. tube, connected electrically to the rear of the can, passes through the center of the entire structure to provide a shielded path for the primary electron beam on its way to the sample. Four electrodes, connected to the grid, to the front of the first channel plate, to the back of the second channel plate, and to a collector anode are located at the side of the housing. Each channel plate is 25 mm in diameter and consists of a honeycomb of about 500,000 electron multiplier channels about 1 mm long and 25 microns in diameter as shown in Figure 3. The channels of each plate are oriented at an angle of 10 degrees with respect to the plate axis, and the plates are oriented so that the channels form a 20 degree chevron structure. In this way it is ensured that incident electrons will strike the channel walls and initiate cascades of secondaries. The counter-acceleration of positive ions is also hindered by this geometry.

Gain

Each of the 500,000 channels of the detector functions as an amplifier, due to the cascading action mentioned above, in much the same way that the photomultiplier
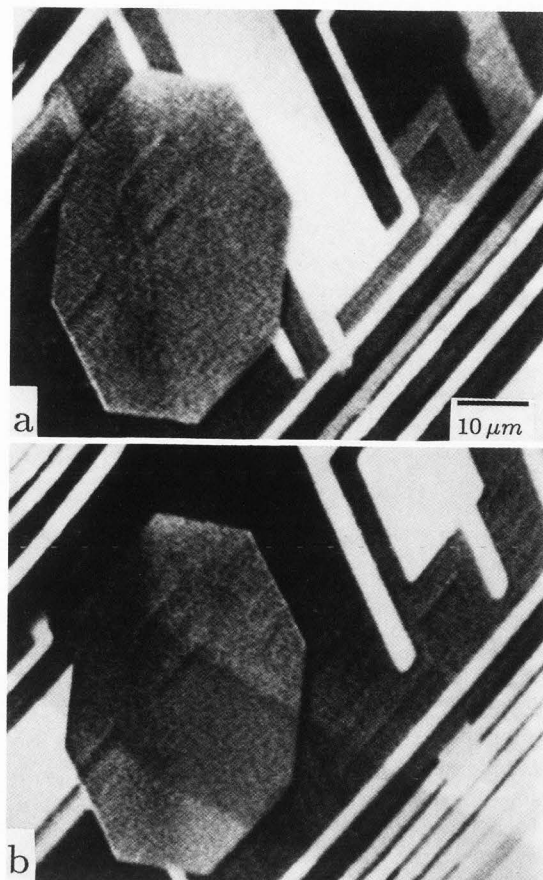

Figure 1. Direct and capacitively coupled voltage contrast images of an operating multilayer microcircuit made with an ET detector. These views were obtained stroboscopically by enabling the primary electron beam for 1 ns during each 600 ns cycle of the chip. The circuit potentials were alternating between 0 and 6 V. The images are the result of integrating many image frames lasting 0.1 s each. Primary beam energy $(E_p) = 750 eV$; primary beam current $(I_P) \cong 1 \ \mu A$ (instantaneous).

does in the Everhart-Thornley detector. The maximum gain of the 3025 MCP is rated by the manufacturer at nearly 10 million when operated with 1000 V across each of the plates. The channel plates are fabricated from a special lead glass as described in [12]. Lead glasses have secondary electron yields, δ, in the range of 2 to 3 with the peaks occurring at primary electron energies in the range of 200 to 450 eV. The gain of a channel may be estimated from the voltage, V, across the channel and the secondary electron yield δ. The gain is $G = \delta^N$ where N is the number of the cascading steps. If one models the continuous channel as a set of N discrete, equal gain stages (as in a photomultiplier), then the electron energy after each stage is $\bar{\epsilon} = V/N$. By using the secondary yield curve of Figure 4a we have estimated the gain for several values of $\bar{\epsilon}$ and $N = V/\bar{\epsilon}$. From the curves of Figure 4b it is apparent that the highest gain occurs at median

energies of about 40eV and this gain corresponds rather well with the gain observed in the 3025 MCP. Apparently the channel length to diameter ratio, which controls N and $\bar{\epsilon}$, was chosen with these considerations in mind.
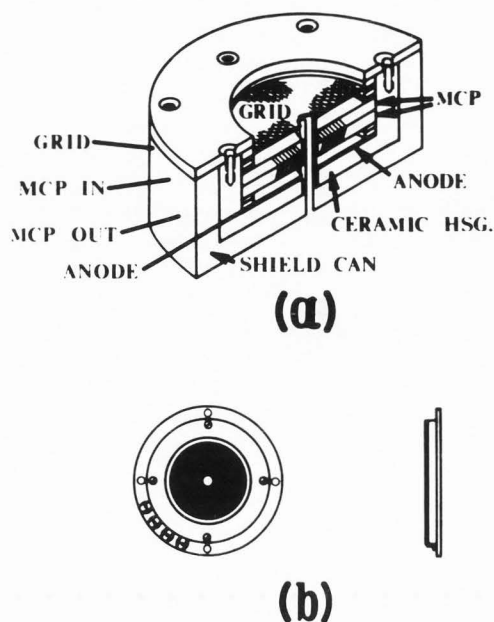

(a)

(b)

Figure 2(a). Cutaway sketch of Galileo model 3025 detector (not to scale).

Figure 2(b). Scale drawing of 3025 detector. Outside diameter $= 55.9\,mm$; total thickness $= 6.0\,mm$.

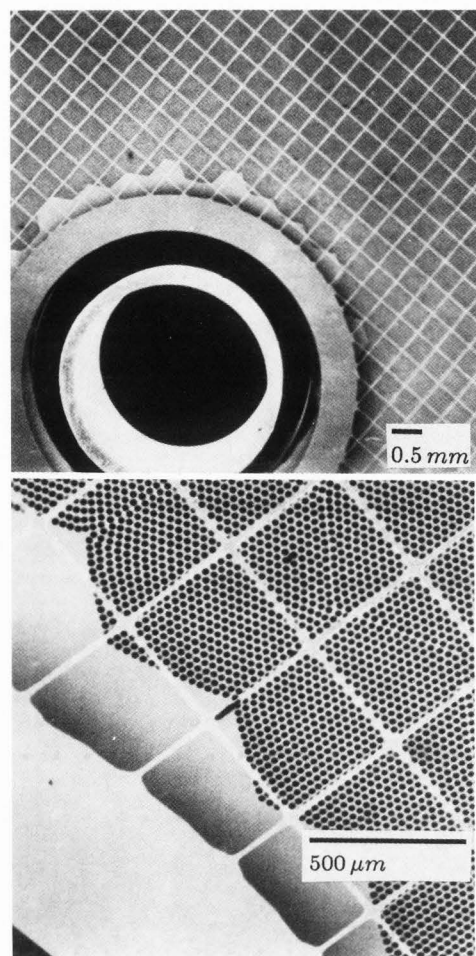(Both drawings, courtesy of Galileo Electro-Optics Corporation.)

Figure 3. SEM photos of the entrance surface of the 3025 detector: (a) near the shielded beam aperture; (b) enlargement showing the 25 micron channels behind the entrance grid. ET detector; exposure time $t_E = 30\ s$; $E_p = 1keV$; $I_p = 200\ pA$

Pulse Width

The spread in the energy of the electrons along the channel corresponds to a time spread in the output pulse and sets a lower limit on the pulse width. Since it takes an electron starting from rest about 150 ps to travel 2 mm under a 2000 V potential drop, one would expect pulse time spreads of this order of magnitude. Pulse widths less than 1 ns have been reported [12]. In fact, the time required for a channel to recover after producing a pulse plays a more important role than pulse width in controlling the rate at which secondary electron data can pass through the MCP. This dead time will be discussed in some detail below.

Lifetime Considerations

The gain of MCP detectors is untroubled by repeated exposure to air, but contamination by back-streaming pump oil, for example, will degrade its operation. Degradation of MCP channels is also associated with erosion of the semiconducting channel lining by electron bombardment; the "electron scrubbing effect" of reference [12]. This deterioration will depend on the output current conditions rather than on the number of counts. Therefore the operating life span can be greatly extended if the MCP is operated at much lower than saturated output current levels. Operation at lower current levels has the additional significant advantage of reducing channel recovery time as we discuss below.

Reports in the literature [12] indicate that the order of 10^{10} total accumulated counts per square millimeter would reduce the gain of a similar detector (operating at maximum gain) by 20%. If this report is accurate, a secondary electron current of 1 pA spread uniformly over the detector surface and counted with 100% efficiency would induce this 20% gain reduction in a 3025 MCP in 220 h. One of the detectors used in this study has been in operation for more than 175 h and is showing no apparent loss of gain, even though it may have suffered some abnormal abuse during testing.
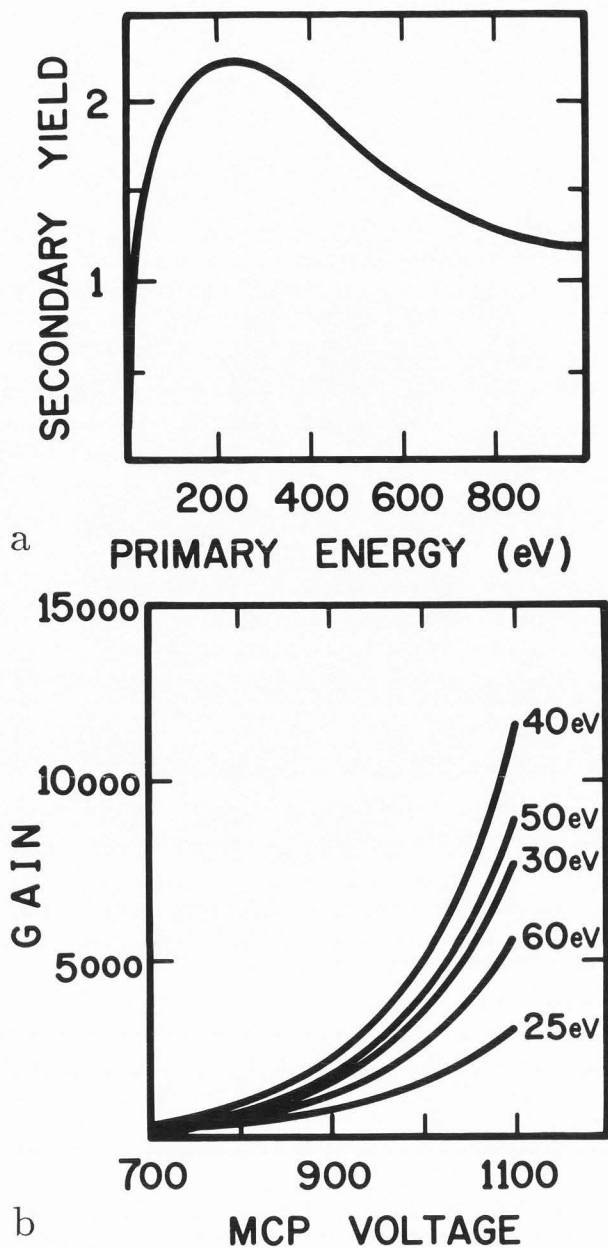
Figure 4. (a) Approximate secondary electron yield (secondary emission current/primary beam current) for lead glass versus primary beam energy. The curve summarizes data found in Dekker (1958), Hachenberg (1950), Kollath (1956) and Wiza (1979). (b) Gain versus applied voltage for several values of the energy increase between cascade stages for a single channel plate.

Experimental Apparatus

The results reported here were obtained on two independent experimental systems. Since both setups were established for multipurpose electron beam experiments,

the results with MCP detection reported here represent early progress rather than fully developed capabilities.

1) A modified ETEC SEM at Clarkson University was equipped with a Galileo 3025 Low Profile MCP. The electrical connections are shown in Figure 5. The detector was suspended from the final lens of the ETEC microscope in a cylindrical aluminum holder. The inner and outer surfaces of the holder were machined coaxially to guarantee alignment of the hole through the detector with the axis of the beam optics. The entrance plane of the detector was 6 mm below the exit plane of the lens. The high voltage and signal leads were led from the aluminum holder through short lengths of quartz tubing to the feed-through connectors normally used for the ET detector. The leads were completely shielded from the beam, sample and detector by an aluminum box.

2) An experimental low-energy SEM at IBM, employing a single-pole type magnetic lens arrangement, uses two electron detectors. One detector is a Galileo 3025 Low Profile MCP mounted as in system 1); the other is a conventional Everhart-Thornley detector.

In system 1) the sample chamber and the detector are free from electric and magnetic fields. In system 2) a coaxially symmetrical magnetic field exists with a flux density which varies according to the focal distance chosen. Some values of the magnetic flux density colinear with the primary beam path are included in Figure 6 where the focal distance is 30 mm and the primary beam energy is 750 eV. The magnetic flux density over the collector grid of the ET detector is inhomogeneous but does not exceed 10^{-3} Tesla.

Detection Efficiency Considerations

Variations in detection efficiencies versus working distance for both detectors are plotted in Figure 6. The amplification factors and scales are independent and arbitrarily chosen for each detector; the data were collected in each case for choices of the amplification which produced the most satisfactory image contrast. It is apparent on the graph that the collection efficiency for both detectors decreases to a very low level, approaching zero with decreasing working distance.

The detection efficiency of the ET detector is seriously affected for working distances much less than 20
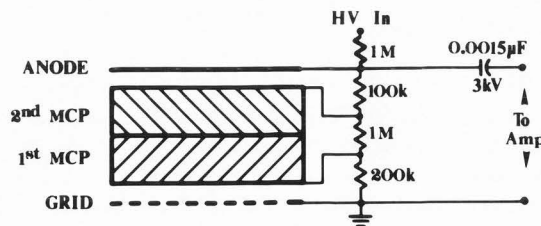

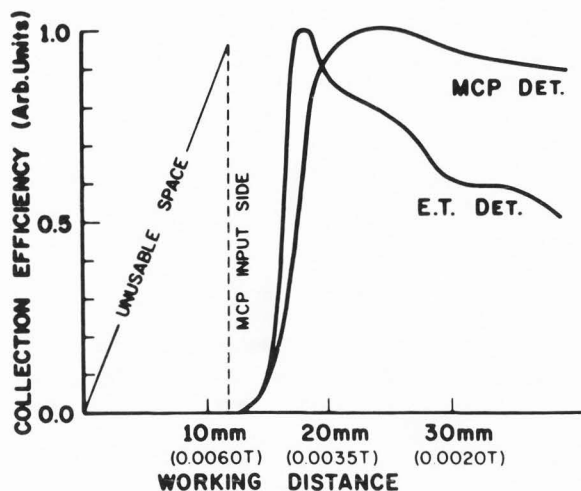Figure 5. Schematic wiring diagram for the 3025 detector.

Figure 6. Collection efficiency versus working distance for the two detectors of system 2. The collection efficiencies for the two detectors are not directly comparable and so were normalized to the same peak value.

mm. This efficiency loss is caused by the energy discrimination properties of the magnetic field gradients, by the increased shielding effects of the pole piece and sample and by the unfavorable detection angles.

For the MCP detector, the abrupt decrease in electron collection efficiency with working distance is associated with the increase in solid angle subtended by the center hole of the MCP and with the increasing focussing effect of the magnetic field on the secondary electrons. At short working distances, the vast majority of the electrons emitted from the sample escape detection as they are funneled into the central hole through the MCP. This efficiency problem at short working distances can probably be reduced by applying a positive bias to the MCP entrance grid which was grounded for the present measurements.

The sample used for these experiments was a square approximately 10 mm on a side and was positioned in all cases perpendicular to the primary beam axis. It was not possible to compare the two detectors using a large un-tilted specimen (e.g., a silicon wafer) because, at reasonable focal distances, most of the ET detector would be obscured by the sample.

Discussion and Results
Dead-Time

It is difficult to calculate accurate time constant values for the MCP detection system because of the distributed nature and unavailability of some of the parameters involved. However, a simple estimate [12] may be based on the associated resistance and capacitance values. We have measured $2.3 \cdot 10^8$ ohms resistance between the electrodes of a 3025 MCP at atmospheric pressure. The reported value for an earlier model 25 mm MCP is

$3 \cdot 10^8$ ohms [12]. Since there are approximately 500,000 channels, the associated resistance per channel is about $1.5 \cdot 10^{14}$ ohms. The capacitance formed between the surface electrodes can be estimated using the following approximations:

1) 50% of the total area between the electrodes is filled with lead glass.
2) The dielectric constant of this glass is $\epsilon = 8.3$.
3) The active area, $A = 4.62 \cdot 10^{-4}$ square meters.
4) The thickness of the glass wafer between electrodes, $t = 1mm$.

The total capacitance between the electrodes then is approximately:

$$
\begin{aligned}
C &= \frac{\epsilon_0 \epsilon A \, (50\%)}{t} \\
&= \left[\frac{(8.85 \cdot 10^{-12} \, F/m)(8.3)(4.62 \cdot 10^{-4} \, m^2)(50\%)}{(0.001 \, m)} \right] \\
&= 17.0 \, pF.
\end{aligned}
$$

The associated capacitance per channel is:

$$
\frac{C}{5 \cdot 10^5} = 3.40 \cdot 10^{-17} \, F.
$$

The time constant, T_c, from the above values is:

$$
\begin{aligned}
T_c &= RC = (1.5 \cdot 10^{14} \, ohms)(3.40 \cdot 10^{-17} \, F) \\
&= 5.10 \, milliseconds.
\end{aligned}
$$

However, even at maximum gain, only the last 20% of the channel length is depleted significantly of charge by the formation of a pulse. Therefore the effective recovery time constant of a channel is approximately 1 millisecond.

From this dead-time figure for a single channel one can estimate the rate at which secondary electrons can be counted by the entire array of channels and hence the minimum time required to record an SEM image. Each channel can count only about 1000 electrons per second, but there are many channels operating independently of one another. While one channel is recovering, other channels are available to deliver pulses to the anode. Thus the array of 500,000 channels, collectively, can count something like $5 \cdot 10^8$ electrons per second if the electrons are distributed uniformly over the array and arrive randomly in time. (More accurately, using Poisson statistics, this incident flux would be counted with 74% efficiency.) This amounts to 80 pA of secondary electrons. Larger secondary currents would be counted with decreasing efficiency due to detector dead-time. Note that the pulse width of about 1 ns described above is a factor of 2 shorter than the expected minimum of 2 ns between pulses due to dead-time.

If the detector delivers pulses at the maximum rate of $5 \cdot 10^8$ per second, then, at one frame a second, a 512 x 512 pixel image would receive an average of $5 \cdot 10^8 / 262{,}144 \cong$ 1900 pulses per pixel. One might suppose that fewer

pulses per pixel would be adequate to form an acceptable image. This supposition is borne out by the micrograph in Figure 7c which was made in 0.3 second with a 20 pA primary beam. If the secondary and primary currents had been equal, there would have been ∼ 140 pulses per pixel available for a 512x512 frame. It seems likely that the secondary flux reaching the detector might, in fact, have been considerably less than 20 pA and that the image of Figure 7c resulted from fewer than 140 pulses per pixel. Since the MCP has a noise figure of about 5 pulses per second (or $6 \cdot 10^{-6}$ pulses per pixel), something less than 140 pulses per pixel is probably quite adequate for a good image. It is interesting to compare the images of Figures 7c and 7f. The latter was obtained in 0.3 seconds under the same conditions with an ET detector.

On account of the very low noise output of the MCP, it appears that one could achieve much faster pixel rates by reducing the MCP gain. At lower gain the depletion of the last 20% of each channel is much less severe and it can be replenished more quickly. With the introduction of the MCP detector, the limiting factor on pixel rate seems to have shifted from the detector to the rate at which primary beam current can be delivered to the sample. Pixel rates several times faster than present TV rates may be possible based on pulse rise-times of less than 500 ps as reported in reference [12].

SEM Images

Following is a discussion of several microphotographs which are included to illustrate the relative performance of the MCP and ET detectors. It should be noted for the comparisons made below that the ET detector could not be deployed to its best advantage. For example, under normal conditions the sample would be tilted toward the ET detector. For the pictures shown here the samples were oriented perpendicularly to the beam. In addition, system 2) produces magnetic fields in the collection volume which adversely affect the ET images.

Figure 7 shows three images made with the MCP (7a, b, c) and three images made with an ET detector. Each of the pairs (a-d, b-e and c-f) were obtained in quick succession under identical conditions. In each case the 750 eV primary beam current was about 20 pA and the exposures decreased from 30 s for a-d, to 3 s for b-e, to 0.3 s for c-f. The working distance was 30 mm with the magnetic field density as indicated in Figure 6. It is conspicuous from the photographs that the signal-to-noise ratio for the MCP detector is significantly better than that for the ET detector. Furthermore, decreasing the exposure time has little effect on the MCP images.

It is interesting to note that the character of the images reflects the differing view points of the two detectors with respect to the illuminating primary beam. The large solid angle of the MCP detector allows it to accept signal from nearly all directions indiscriminately whereas the ET detector is more nearly a point detector. Thus, the straight gold wire in the upper left corner of Figure 7 is nearly obscured in the ET images because of shadowing by the adjacent curved wire. On the other hand, the flat-

tening effect on images which the MCP detector produces may be less pleasing in some instances than the side-lit views provided by the ET detector. Here the spherical character of the gold wire bond is evident in Figure 8a which was made under optimal conditions for the ET detector. In Figure 8b an MCP image of a mesh of round wires has the appearance of woven ribbons.

Conclusions

The present study was motivated by the particular problems associated with acquiring good SEM images with sub-keV primary beams. Chief among these problems is that of transporting a well-focussed beam from the last lens to the sample in the presence of stray electric and magnetic fields. The MCP was evaluated in this context because it would allow the sample to be oriented perpendicular to the beam and therefore to be moved closer to the last lens. So far, this feature of the MCP detector has not been exploited; however, from Figure 6 it is clear that working distances smaller than 20 mm are possible even in a system which has a considerable magnetic field at the sample.

As a result of the study it has become clear that the MCP detector provides additional advantages which suggest its consideration for SEM instruments in general. We have discussed the geometric advantages which permit large planar samples to be mounted and moved conveniently, but it is undoubtedly the electronic characteristics of the detector which are most exciting. With their increased sensitivity, speed and low–noise operation, they promise notable improvements in the rate with which SEM images can be made. This is especially important in applications, as in the semiconductor industry, where images of many different samples must be obtained quickly or where it is necessary to follow rapid changes occurring in a single sample. The capacitively coupled voltage contrast image of Figure 1 is a prime example. On the other hand, imaging speed may be traded for lower primary beam currents. This is of particular value when imaging samples, such as passivated semiconductor devices, whose steady-state surface charge depends on primary beam current density.
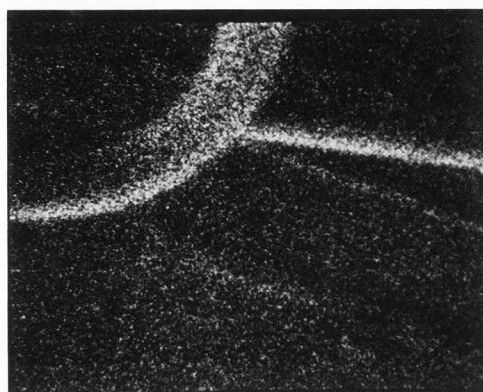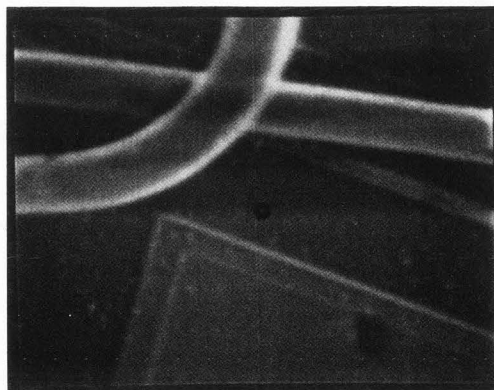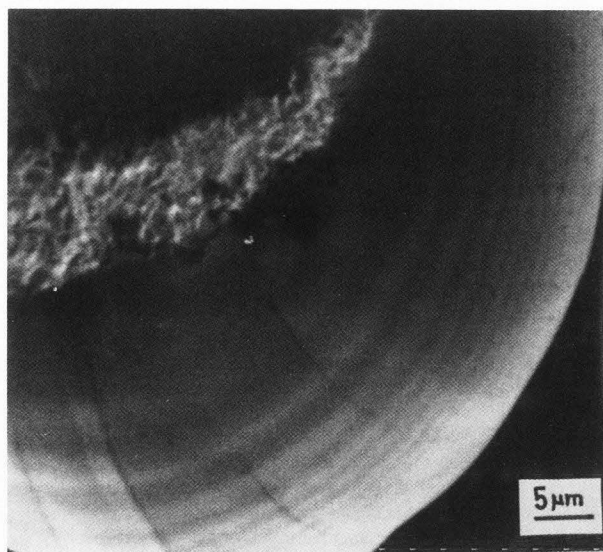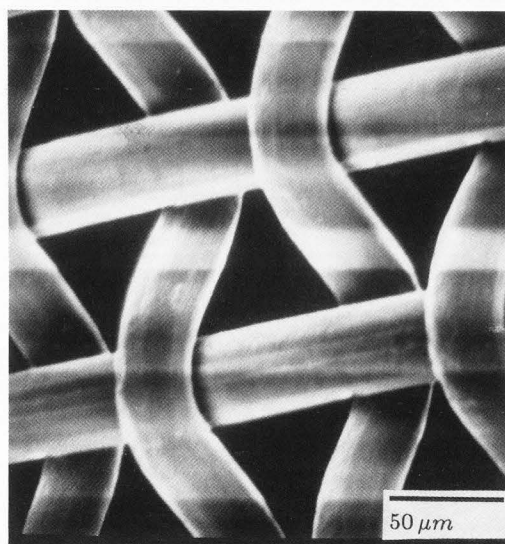
a

20 μm

b

c

d

e
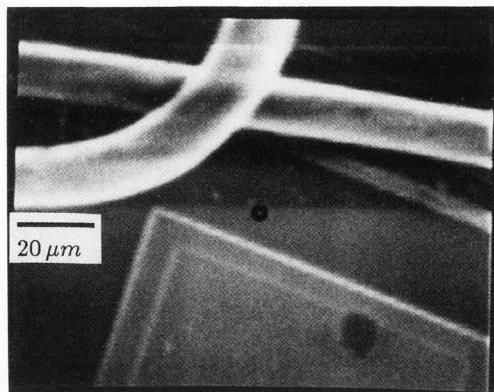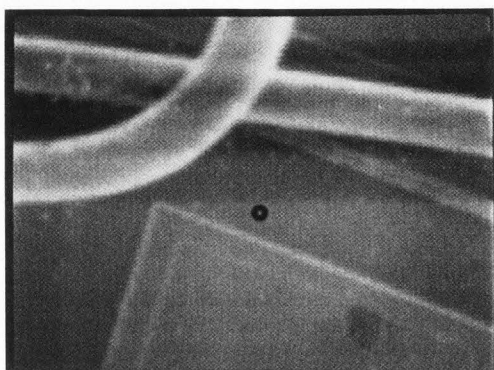
f

Figure 7. Images of microchip bonding wires made with MCP detector (a,b,c) and with ET detector (d,e,f). The top two images (a,d) were obtained in 30 s, the center two in 3 s and the bottom two in 0.3 s; $E_p = 750$ eV; $I_p = 20$ pA.

a

b

Figure 8. (a) View of gold wire bonding pad made with ET detector in system 2 showing the natural three dimensional character of the ET image; $t_E = 180$ s ; $E_p = 750$ eV; $I_p = 20$ pA. (b) View of round wire mesh made with MCP detector in system 1 showing the peculiar flatness caused by the omni-angular electron collection of the MCP; $t_E = 400$ s; $E_p = 2.5$ keV; $I_p = 50$ pA.

References

[1] Dekker AJ (1958), Secondary Electron Emission, Solid State Physics, 6, 251-311.

[2] Everhart TE, Thornley FM (1960) Wide-band detector for micro-microampere low energy electron currents, J. Sci. Instrum., 37, 246-248.

[3] Griffiths BW, Pollard P, Venables JA (1972) A channel plate detector for the scanning electron microscope, Proc. 5th Europe Cong. Electron Microsc. Manchester, Inst. of Physics, Bristol and London, 176-177.

[4] Hachenberg O,Brauer W (1959) Secondary Emission from Solids, Advan. Electron. Electron Phys. 11, 413-499.

[5] Kollath R (1956) Elektronen–Emission Gasentladungen. In: Handbuch der Physik, 21 Springer–Verlag OHG, Berlin, 232-233.

[6] Kotorman L (1980) Non–charging electron beam pulse prober on FET wafers, Scanning Electron Microsc. 1980; IV: 77-84.

[7] Kotorman L (1983) Low energy microscopy utilized in dynamic circuit analysis, IEEE Transactions of Component, Hybrids, and Manufacturing Technology, Vol. CHMJG, No. 4, 527-536.

[8] Robinson VNE (1984) Electron detector used for imaging in the scanning electron microscope. In: Electron Optical Systems, Hren JJ, Lenz FA, Munro E, Sewell PB (eds), SEM Inc, AMF O'Hare IL 60666, 187-195.

[9] Rosch G (1985) A versatile SEM detector with channel plates, Optik Suppl., 1, 60.

[10] Russel PE (1984) Microchannel plates as specialized scanning electron microscopy detectors. In: Electron Optical Systems, Hren JJ, Lenz FA, Munro E, Sewell PB (eds), SEM Inc, AMF O'Hare IL 60666, 197-200.

[11] Russel PE, Mancuso JF (1985) Microchannel plate detector for low voltage scanning electron microscopes, Journal of Microscopy, 140, Pt. 3, 323-330.

[12] Wiza JL (1979) Microchannel plate detectors, Nucl. Instr. and Meth., 162, 587-601.

Discussion With Reviewers

K.L. Lee: The MCP detector set-up described in the paper collects both secondary and backscattered electrons emitted from the sample. The image observed in Figure 8b is close to what one would expect from a backscattered electron detector with a similar set-up. Have you observed any changes in surface details and edge highlights when the entrance grid is biased negatively to suppress the emitted secondaries from entering the detectors? What are the relative contributions to the output signal of the MCP detector, since that is important to voltage contrast applications?

D.J. Dingley: Why don't you show a voltage contrast picture obtained with the MCP detector. The sample should have some level of topography or compositional variation

to see whether the BSE signal will obscure the voltage information from the SE signal?

Authors: The lower portion of Figure A was made with the sample grounded; the upper portion with the sample at +10 V. The marked decrease in picture information with the +10 V bias indicates that the MCP is, in fact, detecting the low energy electrons from which voltage contrast can be obtained. The ratio of the contributions of electrons below 10 eV to those above 10 eV, for the gold wire shown in Figure A, is 1.32 at the primary beam energy of 2.5 keV.
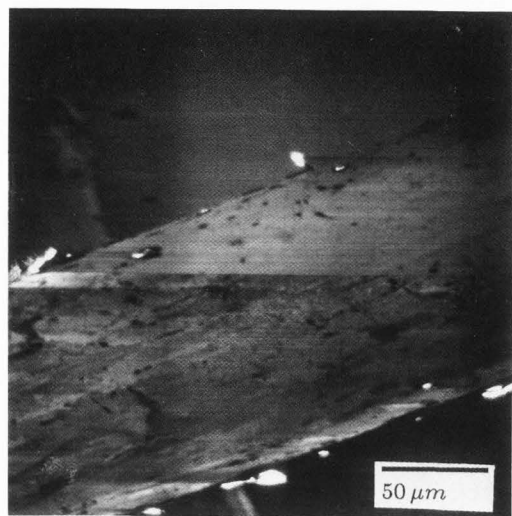

Figure A.   Voltage contrast image of 0.15 mm gold wire made with the MCP detector in system 1. Lower portion with sample grounded; upper portion with sample at +10 V; $t_E = 23$ s; $E_p = 2.5$ keV; $I_p = 50$ pA.

K.L. Lee: What is the detection efficiency of the MCP detector for different electron beam energies incident on the detector? For the collection of low energy secondaries, do you observe any effect of surface contamination on the detector gain?

Authors: For the work reported here, the MCP was operating with the first plate at +200 V with respect to the grounded entrance grid. Thus all electrons strike the first plate with an energy of at least 200 eV. Since this is close to the optimum energy for producing secondary electrons from lead glass, the detector efficiency is nearly independent of the launch speed of secondaries from the sample.